THE APPLICATION OF THE FINITE ELEMENT METHOD TO THE ANALYSIS OF FRACTURE OF CYLINDRICAL SHELLS

Y. ANDO, G. YAGAWA
Department of Nuclear Engineering, The Faculty of Engineering, University of Tokyo, Bunkyo-ku, Tokyo, Japan

K. OKABAYASHI
Power Reactor and Nuclear Fuel Development Corporation, Tokyo, Japan

SUMMARY

In the application of fracture mechanics to the prediction of strength and life of cracked structures, a knowledge of the stress intensification introduced by given defects as a function of applied load and geometry of the structure becomes necessary. The importance of the problem, particularly in the pressure vessel and piping design, is well known and has promoted a great number of research, results of which are gradually adopted in the process of design.

Unfortunately, in the case of complicated geometry such as shell structures with cracks, it becomes extremely difficult to derive an exact solution, especially for a large value of correction factor for the given geometry, which is defined as a function of length of crack, thickness and curvature of a shell. Existing analytical stress intensity factors for the shell structures are the product of analysis for idealized model configurations and loading conditions. In various real situations, however, it is impossible to find suitable model representation for which an exact solution is available. Consequently, in order to evaluate stress intensity factors in such cases it becomes necessary to develop approximate numerical methods.

One such method and its application will now be presented for shell structures. In these five years, various investigators have shown fairly good agreement of stress intensity factors calculated by the finite element method where exact solutions are available. In the first part of this paper, the authors will show some numerical examples for a cracked cylindrical shell which are based on the mixed type finite element method.

An experimental investigation has been performed to show the validity of the computed stress intensity factor to the fracture of the cylindrical shell. The test is conducted on AISI 304 stainless steel pipes with artificial through-thickness crack of 300 and 500 mm length, 316 mm of diameter, 8 mm of wall-thickness and total axial length of 2030 mm. The effect of ambient temperature on the test results is also studied. The objective of the stress intensity factors calculated in the first part of this paper is to provide the theoretical information which can be used in predicting the fracture behavior of shells from that of flat plates and the stress-strain relations by simple tension tests of uniaxial bars under the various ambient temperatures, which may be obtained by relatively simple laboratory tests.

1. INTRODUCTION

In structures, initial flaws or cracks are often contained and developed in service. In the application of fracture mechanics to the prediction of strength and life of cracked structure, a knowledge of the stress field near a crack tip, which is characterized by stress intensity factors, is demanded. The magnitude of stress intensity factors, as is well known, depends upon the geometry of the cracked structures and the type of the applied loads. In most cases , however, exact solutions of the magnitude of stress intensity factors are difficult to obtain. Therefore, approximate numerical technique must be employed to calculate the magnitude. The finite element method is excellent for obtaining stresses and displacements in complex structures and recently attention has been drawn to the application of this technique to fracture mechanics.(1) On the other hand, a number of formulations have been proposed in recent years to predict through-wall critical flaw sizes in cylinder. Eiber et al.(2) reviewed these formulations and concluded from the analysis of the various formulations presented that the most consistant approach for predicting axial critical through-wall flaw sizes in cylindrical shells is the equations proposed by Hahn et al.,(3) In the first part of the present paper, direct method coupled with mixed type finite element technique (4) (5) is used to determine the magnitude of stress intensity factors of the cracked cylindrical shells. Next, the fracture tests of cylindrical shells which contain through-wall cracks are carried out at different environmental temperatures of two kinds. The correlation between the critical hoop stresses thus obtained and the formulation proposed by Hahn et al. is studied in conjunction with the magnitude of stress intensity factors obtained in the first part of the paper.

2. FINITE ELEMENT ANALYSIS OF CRACKED CYLINDRICAL SHELLS

The following calculations are carried out on the basis of the mixed type finite element method for analysis of thin shell structures. In order to calculate the stress intensity factors of cylindrical shells with crack Herrmann's triangular element with 12 freedoms(4) was modified to rectangular element with 16 freedoms.(5) To evaluate the stress intensity factor for opening mode K_1 of mid-surface of the shell, direct method is applied, that is, K_1-value is determined directly from the finite element solution of the stress distributions in the vicinity of crack tip.

2.1 Stress Intensity Factor of Cylindrically Curved Finite Plate

We consider first a finite curved plate with central through-wall crack. The geometry and the finite element idealization of the plate are shown in Figs.1 and 2 respectively. The element used in the analysis is of rectangular shape with no curvature. The calculation is carried out for the following case:

Length of crack $2a=0.8$

Length of the plate in the circumferential direction $2b=2.0$

Length of the plate in the longitudinal direction $2c=2.0$

Thickness of the plate $t=0.1$

Uniform applied stress in the longitudinal direction $\sigma^*_x=1.0$

Poisson's ratio $\nu=0.3$

Consider the membrane stress distribution ahead of the crack in this problem. Providing the curvature of cylinder 1/R in Fig.1 zero and b and c to be long enough compared with a, the stress σ_x ahead of the crack along rhe line of crack prolongation can be expressed as(6)

$$\sigma_x = \frac{\sigma_x^* \sqrt{a}}{\sqrt{2r}} \tag{1}$$

where r is the distance from the crack tip in the prolongation of the crack. Next, let us consider the non-zero case of the curvature 1/R. Fig.3 shows the relation between the stress ratio σ_x^S / σ_x^* and the coordinate r expressed in the logarithmic scale of abscissa and ordinate in which σ_x^S represents the longitudinal stress along the line of crack prolongation in the curved plate. It is noted that the logarithmic stress distributions in this figure are linear with respect to the logarithmic distance from the crack tip and have the common tangent each other including the case of flat plate (i.e. 1/R=0) for the ratio r/a smaller than 0.05~0.1. This implies that the stress ahead of the crack along the line of crack prolongation in the finite curved plate σ_x^S may be written as

$$\sigma_x^S = F \frac{\sigma_x^* \sqrt{a}}{\sqrt{2r}} \tag{2}$$

in which F represents the correction factor which results from the combined effects of curvature and finiteness of the plate and may give some positive number larger than 1. In order to demonstrate the magnitude of these effects, the relation between the correction factor and the curvature of the cylinder for the case of a/b=a/c=0.4 is shown in Fig.4. It should be noted that the finite element solution for zero curvature (i.e. 1/R=0) gives an excellent agreement with Ishida's solution calculated by point matching method.(7) Fig.5 shows the effect of mesh size on the stress intensity factor for opening mode of curved plates K_1, in which K_1 is defined as

$$K_1 = F \sigma_x^* \sqrt{a} \tag{3}$$

The abscissa in this figure represents the size of elements Δr in the line of crack just behind the crack tip to the 5th element from the crack tip along the prolongation of crack, whereas the size of these elements in the direction perpendicular to cracks is always taken 0.008. For R=2.0, the effect of Δr seems negligible, on the other hand for R=0.5 K_1-values decrease linearly with size of element. Thus, for large values of curvature it may be important to use finer mesh in order to obtain reasonable results.

2.2 Pressurized Cylindrical Shell Containing an Axial Crack

Consider a circular cylindrical shell with an axial through-wall crack shown in Fig.6. Radius of the cylinder is R, its wall thickness t and the crack length 2C. The shell is loaded by a uniform pressure p. The finite element program that was used in 2.1 is chosen here and the finite element representation is depicted in Fig.7 which shows developed view of one eighth of the cylinder. To compare the finite element solution with other theoretical ones, the relation between the correction factor F and the parameter for cylindrical shell is given in Fig.8 where λ is defined as

$$\lambda = \left[12(1-\nu^2)\right]^{\frac{1}{4}} \frac{C}{(Rt)^{\frac{1}{2}}} \tag{4}$$

In this figure, Folias' formula(8) is given as follows:

G 5/

$$F = \left[1+1.61\left(\frac{C}{R}\right)^2\left(\frac{R}{t}\right)\right]^{\frac{1}{2}} \tag{5}$$

which is known to be accurate enough only for small values of λ (say $\lambda < 1$). On the other hand Erdogan et al's[9] solution is more acculate than Folias' and gives good approximations up to $\lambda = 8$. The finite element solution gives an excellent agreement with Erdogan et al's up to $\lambda = 4$. For λ bigger than 4, however, the former yields smaller value of F in comparison with the latter, It could be considered that one of the reason of this disagreement is due to the difference of shell theories adopted in these calculations. Next, let us consider an application of Dugdale model[10] to internally pressurized cylindrical shell with an axial crack. Due to the presence of high stresses near the crack tip, plastic flow occurs and a plastic region is developed. This phenomenon leads to the increase of the effective crack length. Following Folias[8], the effective crack length $2C_e^{(1)}$ is determined by the relation:

$$\frac{C}{C_e^{(1)}} = 1 - \frac{3}{4}\left(\frac{\sigma_h}{\sigma_Y}\right)^2\left(\frac{1+1.11\,\dfrac{C_e^{(1)2}}{Rt}}{1+1.11\,\dfrac{(C_e^{(1)}-C)^2}{Rt}}\right) \tag{6}$$

where σ_h is hoop stress due to internal pressure, and σ_Y is yield stress of material. The effective crack length can be obtained by solving eq.(6) for $C_e^{(1)}$. An alternative way of determining the effective crack length is shown in Fig.9, where the plastic zone size ρ is determined as the value of r-coordinate at which the elastic stress perpendicular to the crack coincides with yield stress. The elastic stresses in this method can be calculated by the finite element method. Let this effective crack length be $C_e^{(2)}$. Consider the cylindrical shell containing an axial crack where the radius is 52.1mm, the length of crack is 20mm and the wall thickness is 4mm. Fig.10 shows crack opening displacements computed by applying the finite element method in conjunction with the effective crack lengths discussed above. It should be noted that the crack opening displacement based on $C_e^{(2)}$ gives much smaller value in comparison with that based on $C_e^{(1)}$. The reason of this is apparent because in the calculation based on $C_e^{(2)}$ the stress redistribution due to plastic flow is not considered in determining the plastic zone size.

3. FRACTURE TESTS OF MODEL PIPES MADE FROM STAINLESS STEEL AT AMBIENT TEMPERATURE OF 20°C AND 200°C.

3.1 Material Behaviors of Uniaxial Tension Bar at High Temperature

In order to investigate the material behavior at high temperature, the tension tests of uniaxial bars made from stainless steel AISI 304 are carried out at various ambient temperature ranged from room temperature up to 650°C. To measure temperature of test specimen thermocouples are instrumented at three different places of the specimen and the averaged value of these temperatures is assumed to be the temperature of the specimen tested. At high temperature ceramic gages(K-105A manufactured by Tokyo Sokki Co., Ltd.) are utilized for the temperature up to 370°C, and weldable gages(KH-10-G1 manufactured by Kyowa Dengyo) for the temperature from 450°C up to 650°C, both successfully except at the temperature of 650°C. The results of the test are shown in Fig.11. As for 0.2% yield stress there exist some discrepancies between values measured on drum recorder of the Amsler testing machine and

those of strain gages. In the following chapter the yield stresses based on strain gages will be adopted for the estimation of fracture stress because the former is considered to involve such errors as pin hole distortion and thread elongation.

3.2 Fracture Test of Stainless Steel Pipes Containing Axial Crack

The fracture test of cracked cylinders by internal pressure has been done at the ambient temperature of 20°C and 200°C. The dimensions of the models tested are shown in Fig.12 and Table 1. As can be seen from Table 1, the tests were carried out at two kinds of temperature , i.e. 20°C for specimens 1 and 2, 200°C for specimens 3 and 4. Initial crack is produced by saw cutting, the length of crack is 300mm for specimens 1 and 3 and 500mm for specimens 2 and 4. The cracks are sealed with patches, and instrumented with strain gages ahead of the notch tip. Increasing internal pressure gradually, the sudden initiation of crack was observed at a certain critical pressure. In the present test, the initiation of crack was detected by observing the disconnection of the strain gages instrumented ahead of the notch tip. The test results will be shown in the following chapter accompanied with discussion.

4. DISCUSSION

Following Hahn et al.[3], two formulations valid for different types of toughness and crack length respectively have been proposed. For low-to-medium toughness materials the critical stress intensity factor is given by

$$K_c = \sigma^* \left[\frac{8C}{\pi} \ln \sec \frac{\pi F \sigma_h}{2\sigma^*} \right]^{\frac{1}{2}} \tag{7}$$

whereas for high toughness materials the flow stress formula:

$$\sigma^* = \sigma_h F \tag{8}$$

holds when the yield stress criterion

$$\left(\frac{K_c}{\sigma_Y} \right)^2 / C \geq 7 \tag{9}$$

is satisfied. In the above, σ_h is the critical hoop stress and σ_Y is yield stress. On the other hand the flow stress σ^* is defined as

$$\sigma^* = 0.51(\sigma_Y + \sigma_u) \tag{10}$$

where σ_Y may be related with the 0.2% yield stress of stainless steel $\sigma_{0.2}$ by

$$\frac{2}{3}\sigma_Y = 0.9\,\sigma_{0.2} \tag{11}$$

due to the fact that in ASME USAS B31.7[11] $\frac{2}{3}$ x yield stress of ferritic alloy steel is considered to be equivalent to 0.9 x $\sigma_{0.2}$ of austeritic stainless steel. Table 2 presents the solution of eq.(8), in which the correction factor F is calculated by the finite element method presented in this paper because, for large values of λ such as 13 which corresponds to the crack in the present test, the correction factor is not available by any analytical means. The agreement between $\sigma_h F$ and σ^* is surprisingly good for any test specimen as is shown in Table 2. The yield stress criterion given by eq.(9) is satisfied except for specimen 2.

REFERENCES

(1) GALLAGHER, R.H., Survey and Evaluation of the Finite Element Method in Linear Fracture Mechanics Analysis, 1st Int. Conf. Struct. Mech. Reactor Technol., Part L, 637-653(1972).

(2) EIBER, R.J. et al., Review of Through-Wall Critical Crack Formulations for Piping and Cylindrical Vessels, Battelle Memorial Institute, Columbus, Ohio, BMI-1883(1970).

(3) HAHN, G.T. et al., Criteria for Crack Extension in Cylindrical Pressure Vessels, Int. J. Fracture Mech., Vol.5, 187-210(1969).

(4) HERRMANN, L.R. and CAMPBELL, D.M., A Finite-Element Analysis for Thin Shells, AIAA J., Vol.6, 1842-1847(1968).

(5) ANDO, Y. et al., Stress Distributions in Thin-Walled Intersecting Cylindrical Shells Subjected to Internal Pressure and In-Plane Force, 1st Int. Conf. Stract. Mech. Reactor Technol., Part G, 123-136(1972).

(6) PARIS, P.C. and SIH, G.C., Stress Analysis of Cracks, Fracture Toughness Testing and Its Applications, ASTM-STP-381, 30-83(1965).

(7) ISHIDA, M., Method of Laurent Series Expansion for Internal Crack Problems, Mechanics of Fracture,Vol.1, Method of Analysis and Solutions of Crack Problems Edited by G.C. SIH, Noordhoff Int. Pub. Leyden(1973).

(8) FOLIAS, E.S., An Axial Crack in a Pressurized Cylindrical Shell, Int. J. Fract. Mech., Vol.1, 104-113(1965).

(9) ERDOGAN, F. and KIBLER, J.J., Cylindrical and Spherical Shells with Cracks, ibid., Vol.5, 229-237(1969).

(10) DUGDALE, D.S., Yielding of Steel Sheet Containing Slits, J. Mech. Phys. Solids, Vol.8, 100-104(1960).

(11) USA Standard Code for Pressure Piping, Nuclear Power Piping USAS-B31.7, ASME(1969).

Table 1. Dimensions and material properties of test specimens

TEST NUMBER	AMBIENT TEMPERATURE (°C)	0.2% YIELD STRESS $\sigma_{0.2}$(kg/mm^2)*	TENSILE STRENGTH σ_u(kg/mm^2)*	DIAMETER OF CYLINDER 2R(mm)	WALL THICKNESS OF CYLINDER t(mm)	CRACK LENGTH 2C(mm)	SHELL PARAMETER λ
1	20	24.5	62.9	308	8	300	7.8
2	20	24.5	62.9	308	8	500	13.0
3	200	16.2	46.1	308	8	300	7.8
4	200	16.2	46.1	308	8	500	13.0

* Obtained from Fig.11

Table 2. Summary of results

TEST NUMBER	CRITICAL HOOP STRESS σ_h(kg/mm^2)	CORRECTION FACTOR F	FLOW STRESS σ^*(kg/mm^2)	σ_{hF}/σ^*	$\left(\frac{K_c}{\sigma_Y}\right)^2 / C$
1	12.5	3.84	48.0	1.00	7.2
2	8.8	5.35	48.0	0.98	6.6
3	9.5	3.84	34.0	1.07	9.7
4	6.5	5.35	34.0	1.02	8.2

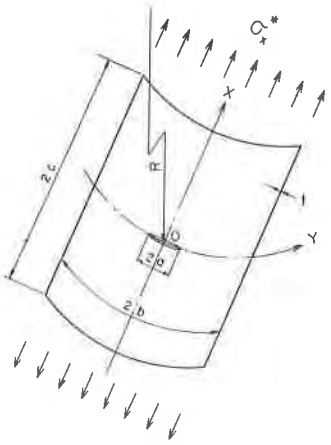

Fig.1 Curved plate with a central through-wall crack under uniform tension.

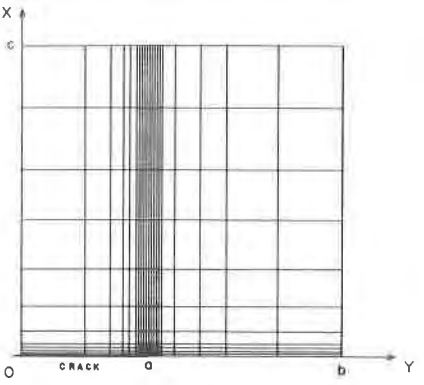

Fig.2 Finite element idealization of a quarter of the cracked plate.

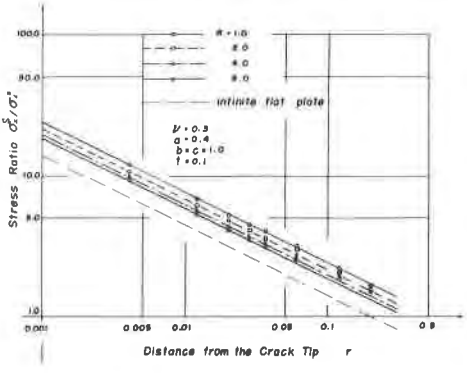

Fig.3 The loggrithmic expression of the relation between the stress ratio σ_x^s / σ_x^w and the coordinate r.

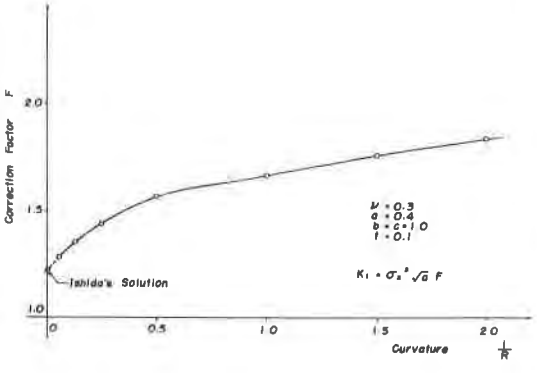

Fig.4 The relation between the correction factor F and the curvature of the cylinder 1/R.

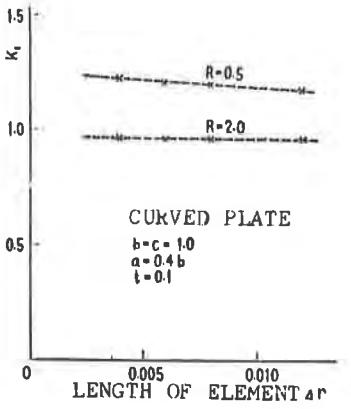

Fig.5 The effect of mesh size on the stress intensity factor K_1.

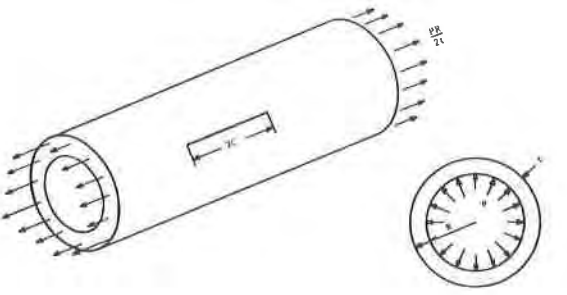

Fig.6 Circular cylindrical shell with through-wall axial crack under internal pressure.

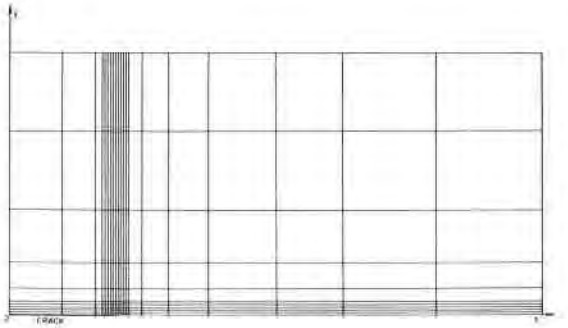

Fig.7 Finite element idealization of one eighth of the cylindrical shell.

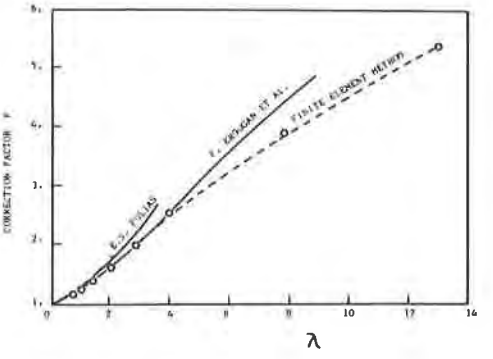

Fig.8 The relation between the correction factor F and the shell parameter λ

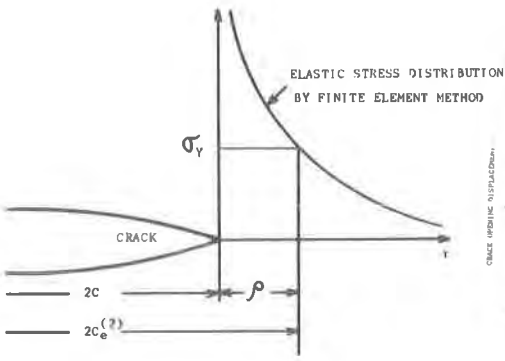

Fig.9 A method of determining the effective crack length of the cylindrical shell.

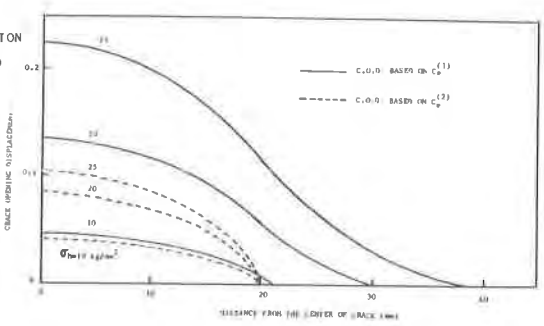

Fig.10 Crack opening displacements of the cylindrical shell containing an axial crack.

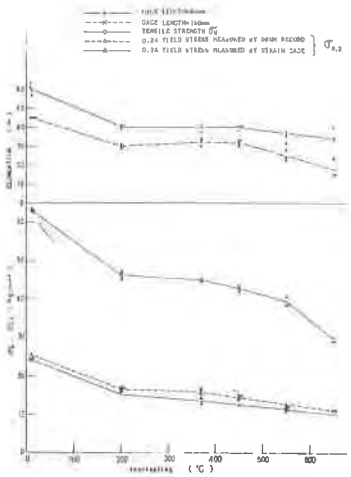

Fig.11 Results of the uniaxial tension test.

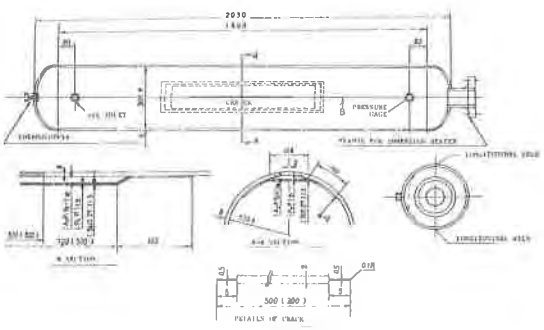

Fig.12 The dimensions of the pipe model.